Estuaries and Coasts Vol. 29, No. 1, p. 72–80 February 2006

Modeling Nonlinear Seagrass Clonal Growth: Assessing the Efficiency of Space Occupation across the Seagrass Flora

TOMÀS SINTES[1], NÚRIA MARBÀ[2,*], and CARLOS M. DUARTE[2]

[1] *Departament de Física, Universitat Illes Balears, 07122 Palma de Mallorca, Spain*
[2] *IMEDEA (CSIC-UIB), Grup d'Oceanografia Interdisciplinar, Institut Mediterrani d'Estudis Avançats, C/ Miquel Marquès 21, 07190 Esporles, Spain*

ABSTRACT: The clonal growth of 9 seagrass species was modeled using a simulation model based on observed clonal growth rules (i.e., spacer length, rhizome elongation rates, branching rates, branching angle) and shoot mortality rates for seagrass species. The results of the model confirmed the occurrence of complex, nonlinear growth of seagrass clones derived from internal dynamics of space occupation. The modeled clones progressed from a diffuse-limited aggregation (DLA), dendritic growth, identified with a guerrilla strategy of space occupation, to a compact (Eden) growth, comparable to the phalanx strategy of space occupation, once internal recolonization of gaps, left by dead shoots within the clone, begins. The time at which seagrass clones shifted from diffuse limited to compact growth was predictable from the branching angle and frequency of the species and varied from 1 yr to several decades among species. As a consequence the growth behavior and the apparent growth strategy of the species changes with the development of the clones. The results of the model demonstrate that the emergent complexity of seagrass clonal growth is contained within the simple set of growth rules that can be used to represent clonal growth.

Introduction

Clonal growth has been identified as the primary component of the productivity of seagrasses, with population dynamics depending on the continuous formation of new modules through meristematic activity (Tomlison 1974). In addition to its role in the maintenance of established populations, the space occupation by most seagrass species is closely dependent on clonal extension (Duarte and Sand-Jesen 1990; Marbà and Duarte 1998; Hemminga and Duarte 2000). Since clonal growth can be described parsimoniously through a few rules (the distance between consecutive shoots along the rhizome or spacer length, the linear extension rates of the rhizomes, and their branching rate and angle; Bell and Tomlinson 1980; Marbà and Duarte 1998), there has been a considerable effort to assess clonal growth rules across the seagrass flora (Marbà and Duarte 1998; Hemminga and Duarte 2000).

The results delivered by this research have revealed a broad range of variation in all clonal growth rules, with linear rhizome extension rates and branching rates varying up to two orders of magnitude across the seagrass flora and the branching angle ranging from shallow (about 20°) to broad (about 80°) across species (Marbà and Duarte 1998). The research conducted has shown these growth rules to be scaled to the size of the seagrass species with the smaller species showing the fastest linear extension rates, high branching frequency and broad branching angles (Marbà and Duarte 1998).

The capacity to describe clonal growth from a few rules has led to efforts to model space occupation by plant clones. Most efforts so far have been directed to produce visual representations of clonal networks of land plants (Bell 1979; Bell and Tomlinson 1980; Brouns 1986; Callaghan et al. 1990; Molenaar et al. 2000). Application of such models to seagrasses have evolved to simple models (based on linear extension rates or rate of advance of vegetation front) to produce rough predictions of colonization time scales (Duarte 1995; Kendrick et al. 1999; Fonseca et al. 2004) and to examine early seagrass space occupation by seagrass clones (Marbà and Duarte 1998). A diffusion-driven model of space occupation by seagrass clones has been developed more recently and tested for *Cymodocea nodosa* (Sintes et al. 2005). In a diffusive-driven model new units diffuse to join the cluster, or are added, at the tips of the branches (Bunde and Havlin 1996) of the network. This diffusive-driven model, which allows the visualization and analysis of space occupation by seagrass clones over long time scales, has provided evidence of nonlinear growth dynamics in seagrass clones, explaining observations of such phenomena for *C. nodosa* patches (Vidondo et al. 1997). Despite *C. nodosa* clones growing according to the same growth rules during their life span, young clones develop according to diffusive-limited aggregation (DLA) processes (Bunde and Havlin

* Corresponding author: tele: +34 971 611720; fax: +34 971 611761; e-mail: nuria.marba@uib.es

TABLE 1. Parameters used as model input for each of the species simulated [mean (SD)] and the time over which clonal growth was simulated. Data from Olesen and Sand-Jensen (1994): *Zostera marina*, Vermaat et al. (1995): *Enhalus acoroides* and *Halodule uninervis*, Marbà et al. (1996): *Posidonia oceanica*, Marbà and Duarte (1998): branching angles for all species but *Cymodocea nodosa*, Marbà and Walker (1999): *Posidonia australis*, *Anphibolis antarctica*, and *Heterozostera tasmanica*, Duarte et al. (1996): *Thalassodendron ciliatum*, and Sintes et al. (2005): *C. nodosa*. The minimum and maximum cut off values used in the model are shown below the mean (SD) as min:max.

Species	Spacer length: ρ (cm)	Rhizome elongation: v (cm yr^{-1} $apex^{-1}$)	Branching rate: ν_b (branches yr^{-1} $apex^{-1}$)	Branching angle: Φ (degrees)	Mortality rate: μ_r (units yr^{-1})	Simulated time (yr)
E. acoroides	6.55 (1.14)	3.10 (2.20)	0.261 (0.002)	56.5 (1.6)	0.23 (0.05)	500
	4.5:8.5	0.0:6.5	0.24:0.28	25:80	0.12:0.35	
P. oceanica	2.87 (0.87)	6.11 (0.06)	0.06 (0.02)	49.0 (2.0)	0.156 (0.11)	400
	1.0:5.0	5.0:7.0	0.0:0.12	20:80	0.04:0.35	
P. australis	6.00 (0.48)	9.31 (0.29)	0.524 (0.005)	20.8 (1.7)	0.37 (0.03)	125
	2.0:10.0	7.0:11.0	0.4:0.6	5:35	0.30:0.50	
A. antartica	3.86 (0.21)	20.23 (14.77)	0.168 (0.002)	48.3 (1.6)	0.58 (0.08)	125
	1.0:6.0	2.0:40.0	0.14:0.19	25:75	0.40:0.75	
T. ciliatum	3.32 (0.64)	17.25 (1.42)	0.422 (0.004)	30.7 (1.7)	0.71 (0.04)	100
	2.0:5.0	12.0:22.0	0.35:0.50	10:50	0.65:0.80	
H. uninervis	2.72 (0.59)	101.17 (36.39)	0.452 (0.005)	55.3 (1.2)	1.81 (0.42)	100
	0.5:5.0	50.0:150.0	0.35:0.55	25:75	1.0:2.6	
Z. marina	5.14 (0.24)	26.12 (2.60)	1.587 (0.016)	66.7 (2.2)	1.27 (0.20)	30
	2.0:8.0	22.0:30.0	1.1:2.1	30:100	0.8:1.8	
C. nodosa	3.7 (0.1)	160.0 (5.0)	2.30 (0.05)	46.0 (1.5)	0.92 (0.08)	15
	2.5:5.0	140.0:180.0	1.0:3.5	10:80	0.7:1.1	
H. tasmanica	2.07 (0.08)	102.82 (47.18)	7.69 (0.08)	56.0 (1.9)	3.71 (0.56)	12
	1.0:3.0	30:170	5.0:9.0	35:75	2.5:5.0	

1996), dominated by branching pattern, whereas the spread of older clones occur at the periphery of the clone according to the Eden process (Jullien and Botet 1985), typical of growth compact structures. Although the model developed was tested with *C. nodosa*, the principles contained in this model are generic to all seagrass species and can be applied to examine the dynamics and efficiency of space occupation across the seagrass flora.

Here we use the diffusion-driven model developed by Sintes et al. (2005) to examine the dynamics and efficiency of space occupation by clonal growth across the seagrass flora. We do so by running the model for a subset (9 species) of the seagrass flora, encompassing the broad range of clonal growth rules (spacer length, rhizome elongation rates, branching rates, and branching angle) present in the flora, for which sufficient empirical data exist. The model uses available estimates of shoot mortality rates for the modeled species.

Materials and Methods

The numerical model developed (Sintes et al. 2005) is inspired by pattern growth formation models developed within the realm of material sciences and we briefly review it here. The model is initiated by placing a seed (a shoot holding an apical meristem) at an origin coordinate r_0 and assigning to it a unitary, randomly-oriented, vector director u setting the direction of the rhizome extension. The model then uses observed growth rules (i.e., spacer length [ρ], linear rhizome elongation rate [v], and branching rate [ν_b] and angle [Φ], Table 1), characterized by their average and standard deviation, including a cutoff at the minimum and maximum observed values, which were sampled at each time step from the corresponding gaussian distribution, accounting for the variability within seagrass species. The model iterates the clonal growth process according to the following steps.

A rhizome that originates in the apex is proposed to grow from r_0 to $r = r_0 + \rho u$.

A time step Δt is defined corresponding to the time interval for a rhizome apex to produce two consecutive shoots. The time step is evaluated as: $\Delta t = \rho/(vN_a(t))$. $N_a(t)$ is the number of apices present in the model at time t.

At each time step, the probability of branching for each rhizome meristem is also evaluated (Sintes et al. 2005). The branching probability is calculated as the product $\nu_b \times \rho \times v^{-1}$ where v is the rhizome elongation rate (cm $apex^{-1}$ yr^{-1}).

The model also uses the mortality rates of the shoots (μ_r) to evaluate the probability that each individual shoot will survive to the next time step. Within a time step Δt, $\mu_r \times \Delta t$ shoots are removed from the clone.

The model tracks the fate of all individual shoots and rhizome meristems produced along the clone development to yield a spatial representation of the clone at various time steps. The model output also contains descriptors of the evolution of the relevant variables describing patch growth, such as the total length of the rhizome network, the patch radius, the internal density of shoots and rhizome apices, and the linear patch growth rate.

The size of the modelled growing patch at any time t is measured through the evaluation of the radius of gyration $R_g(t)$, defined as:

$$R_g(t) = \sqrt{\frac{1}{N_s(t)} \sum_{i=1}^{N_s} (r_i(t) - r_{CM})^2} \qquad (1)$$

where $r_i(t)$ is the position of the ith shoot at time t, r_{CM} denotes the position of the center of mass of the patch, and $N_s(t)$ is the number of living shoots in the patch. The radius of gyration, a quantity used to characterize the linear dimension of objects in most growth models developed in the context of physics (Stanley and Ostrowski 1986), is equivalent to the circular-equivalent radius weighed for the internal distribution of shoot density of the patch. The use of the radius of gyration to characterize patch size is particularly useful at the initial stages of growth, when the patches present highly irregular shapes and internal densities (Sintes et al. 2005). The linear patch growth rate is calculated as the time derivative of the radius of gyration.

The internal density of the patch is calculated through the evaluation of the average number of shoots and apices in a square cell of size 20×20 cm^2, comparable to the field estimation of shoot density. The correct simulation of the internal density by the model required consideration of a per capita area equivalent to the distance between consecutive shoots setting an upper limit to an exclusion area where only one shoot may grow, avoiding the same position to be simultaneously occupied by more than one shoot (Sintes et al. 2005). The magnitude of the exclusion area was defined empirically, by fitting this parameter in the model as to achieve the shoot density reported in natural stands of the species tested. The robustness of the empirically-fitted exclusion area was supported by the observation that the resulting density of rhizome apices in the original model, which is independent of the fitting procedure, matched field observations.

The model was used to simulate and compare clonal development for 9 seagrass species, for which the input data required are available (Table 1). For each species, the model was run with sufficient time steps to achieve a steady-state clonal growth, which varied from 12 to 500 yr among species (Table 1). The model output values presented here are average estimates obtained over the development of 50 replicated clones, and they yield estimates of the average structure of the clones at each time step for each of the 9 species examined.

The model followed the fate and position of each individual shoot and rhizome apices, involving several million shoots and tens of thousands of apices by the time the model stopped. The model was written in Fortran and was run on a workstation. The run of these models required massive storage space (512 Mb of memory space for each species) and (CPU) time (typically about 10 d of CPU time on a Pentium III at 1 GHz).

Results

The model predicted the development of the shoot and apex density of the clones of the species simulated, showing an initial phase of rapid increase to reach a steady state at times ranging between < 1 yr for the fastest growing species (*Heterozostera tasmanica*) and > 100 yr for the slowest growing species (*Enhalus acoroides*; Fig. 1). The effective linear extension rate of the clones also increased rapidly with time to reach steady-state growth rates, similar to the rhizome extension rates of the species (Table 1), after an elapsed time ranging from < 2 yr for the fastest growing species (*C. nodosa*) to 50 yr for the species with the slowest growing rhizomes (*Posidonia oceanica*; Fig. 2). The total size of the clonal networks, as described by the total number of living shoots and the total rhizome length produced by any one time step, showed an initial exponential growth along the first 1/3 of the simulation period for each species, and grew much slower thereafter (Fig. 3). The growth efficiency of the clones, as described by the ratio between the size of the clone (radius of gyration) and the total rhizome length, declined with time (Fig. 4), so that young, small clones occupy space much more efficiently, per unit rhizome produced, than large clones reaching steady-state growth, with efficiency only about 0.1% of that at the initial phases of clonal extension.

These results indicate the growth of seagrass clones to be strongly nonlinear, with a rapid initial growth followed by a reduction in growth as the clones reach steady-state growth equivalent to the rhizome extension rate (Figs. 1–4, Table 2). The aspect of the seagrass clones also changes during its development from rather diffuse, indented patches to compact structures (Fig. 5). The time at which the growth switches from the rapid initial phase to the steady-state growth characteristic of compact clones (i.e., the time at which the slope of the change in the number of living shoots and the growth rate with time switches) differed greatly between species, ranging from < 1 yr for the species showing the fastest clonal development (*H. tasmanica*) to 90 yr for the species with the slowest clonal development (*P. oceanica*; Table 2).

The nonlinear growth of the clones is also evident in the examination of the relationship between the radial patch size and the number of living shoots in the clones (Fig. 6). Two regions of distinct slopes in the relationship between the radial patch size and

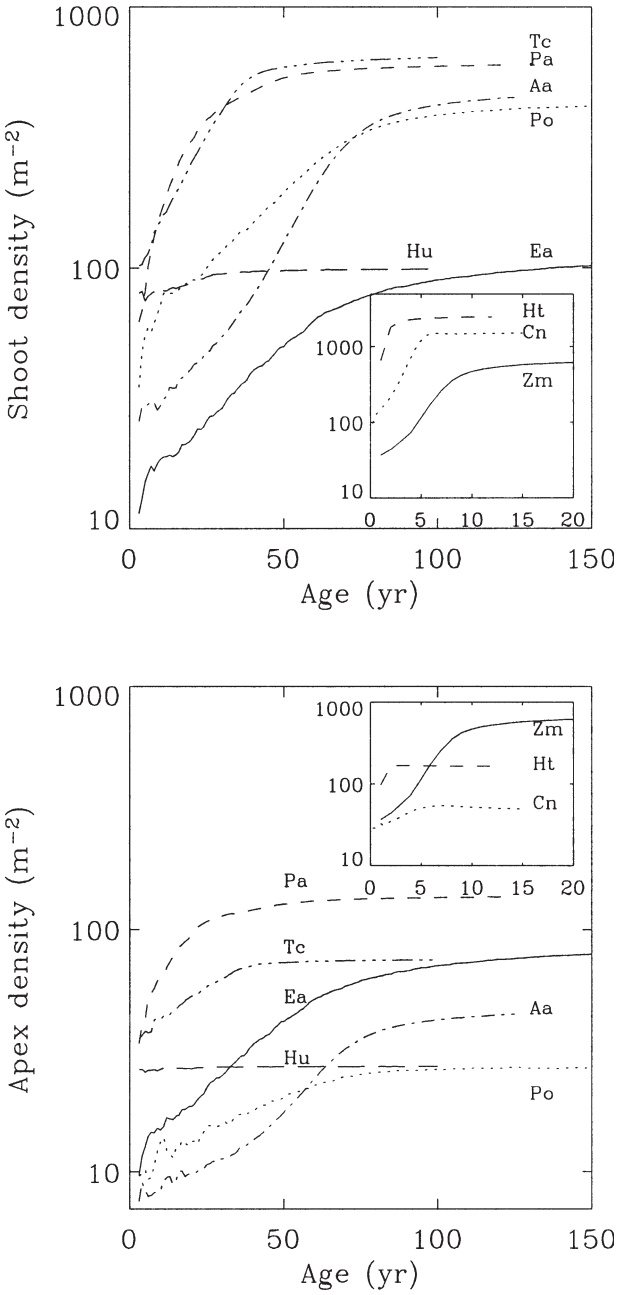

Fig. 1. Shoot density profiles and apex density profile versus patch age. The different lines correspond to the different species under study. The inset plot includes the corresponding densities for the fastest growing species. The labels stand for: Ea = *Enalus acoroides*, Po = *Posidonia oceanica*, Pa = *Posidonia australis*, Aa = *Amphibolis antartica*, Tc = *Thalassodendrom ciliatum*, Hu = *Halolude uninervis*, Zm = *Zostera marina*, Cn = *Cymodocea nodosa*, and Ht = *Heterozostera tasmanica*.

the number of living shoots can be defined: a region where radial patch size increases as the 0.6 power of the number of living shoots, characteristic of patches with $<$ 1,000 shoots; and a region where

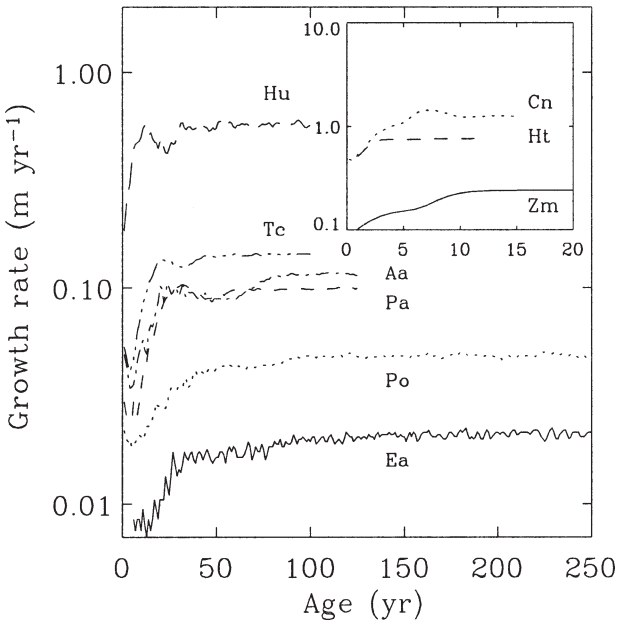

Fig. 2. Patch growth rate versus age for the different species studied. Labels identify the species as in Fig. 1.

radial patch size increases as the 0.5 power of the number of living shoots, characteristic of compact clones (Figs. 5 and 6).

Discussion

The model used predicts the simple growth rules used to simulate clonal growth to lead to nonlinear clonal growth, as reported for *C. nodosa* (Vidondo et al. 1997; Sintes et al. 2005). Seagrass patches evolve from highly diffuse, dendritic structures to compact structures along the growth process (Fig. 5). The common behavior observed in all the species studied, despite their differences in size and clonal growth rules (Table 1), demonstrates that the nature of the emergent complexity is contained within the simple set of growth rules that can be used to represent clonal growth (Marbà and Duarte 1998; Sintes et al. 2005).

The nonlinear behavior of clonal growth depicted by the model derives from a regime shift in the growth mode of the clones from a DLA process to a compact growth mode as the shape of the clones shift from dendritic to compact structures. These changes are associated with a major reduction in the efficiency of space occupation despite accelerated net linear extension rates along the growth process. The compact structures formed by developed clones and the sharp decline in growth efficiency result from internal space limitation, reflected in the maintenance of steady-state shoot density and the fact that much of the rhizome growth of the clonal network is invested in recolonizing internal spaces

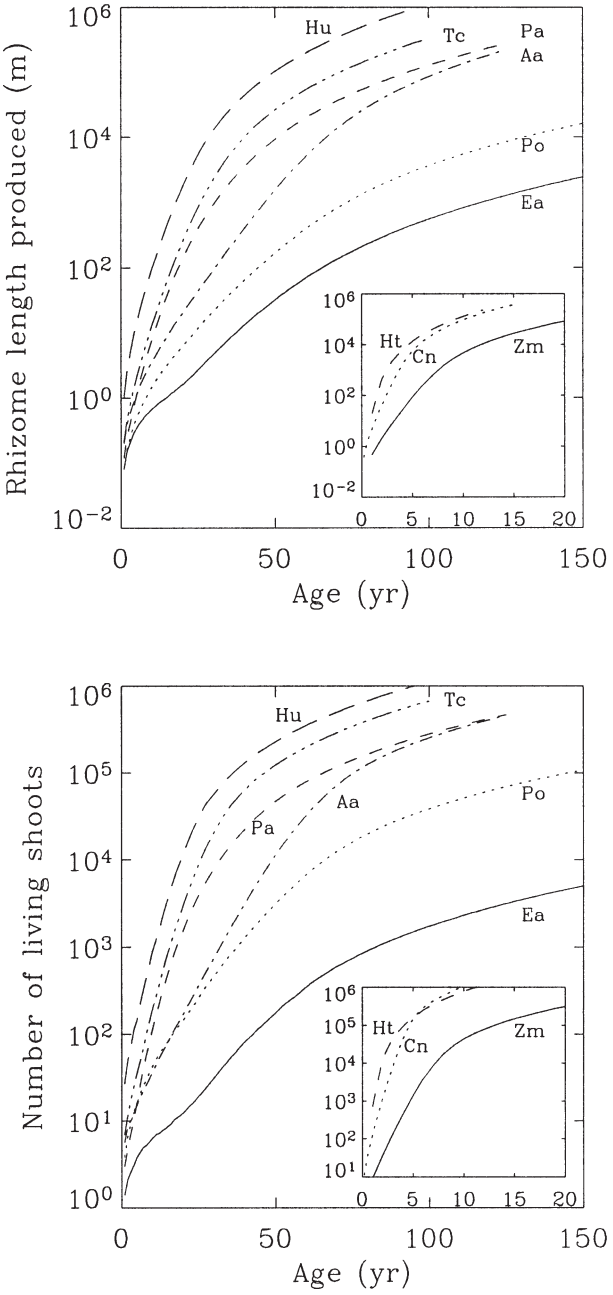

Fig. 3. Total rhizome length produced by the clone and number of living shoots in the clone versus patch age for the different species studied. Inset plots include the behavior of the fastest growing species. Labels identify the species as in Fig. 1.

left void by shoot mortality. Most of the rhizome material produced by young clones results in the effective extension of the clone, leading to the high early growth efficiency highlighted by the model.

During the early stages of patch growth, the branches basically grow independently of each other. During this growth regime, the change in

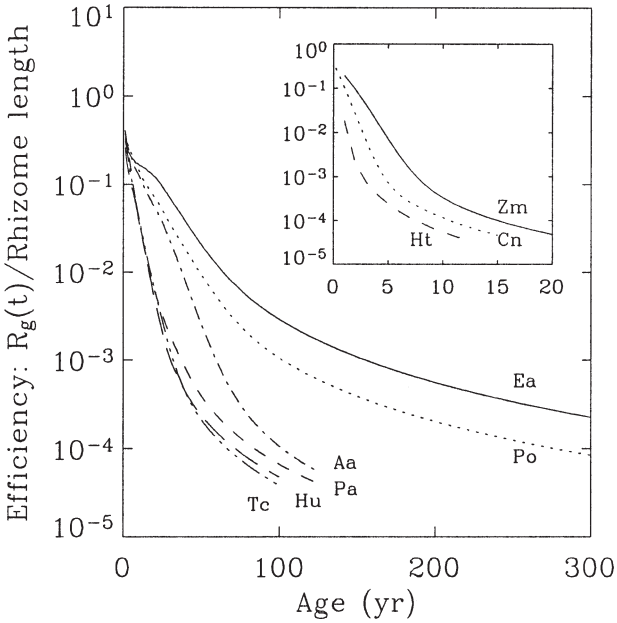

Fig. 4. Efficiency of space occupation profile versus patch age for the different species studied. The inset plot includes the behavior of the fastest growing species. Labels identify the species as in Fig. 1.

the number of apices N_a and living shoots N_s, is controlled by two ordinary differential equations:

$$\begin{aligned} \frac{dN_a}{dt} &= \nu_b N_a \\ \frac{dN_s}{dt} &= -\mu_r N_s + N_a \end{aligned} \tag{2}$$

where ν_b and μ_r are the branching rate and mortality rate, respectively, of the species. The solution can be readily derived (cf., Sintes et al. 2005) showing that both the change in the number of shoots $N_s(t)$ and apices $N_a(t)$ is an exponential process dominated by the branching rate ν_b,

$$N_s(t) \sim N_a(t) \sim \exp(\nu_b t) \tag{3}$$

This is also the case for the overall length of the clonal network produced, which is proportional to the number of shoots. The validity of this theoretical prediction derived from the analysis of the growth process (Eq. 3), and the hypothesis of independent branching rate, can be easily checked by measuring the observed branching rate of our model outputs for the different seagrass species under study. The observed ν_b during the early growth stages is obtained by computing the slopes of the curves corresponding to the rhizome length produced and number of living shoots in a semi-log representation (Fig. 3). The results show a reason-

TABLE 2. Comparison between the branching rate (ν_b) model data input (Table 1) and that calculated as the initial slope between the total number of shoots produced by the clone and clonal age (Fig. 3); the exponent characterizing the power law behavior for the radial patch size versus the number of living shoots for small clones $\alpha^\dagger$ (DLA process), and large clones $\alpha^\ddagger$ (compact radial growth) (Fig. 4.); the efficiency decay rate (η) predicted from the measured exponent α and the branching frequency ν_b, and the rate of decline derived from the model output (Fig. 4); and the age at which the clones undergo regime shift (τ) predicted from the branching angle (in radians) and branching rate, and that derived from the model output. Data includes average (± SE) of model output for each species.

Species	ν_b (model input) (branches yr^{-1} $apex^{-1}$)	ν_b (calculated)	$\alpha^\dagger$	$\alpha^\ddagger$	Efficiency decay rate: $\eta = (\alpha - 1)\ \nu_b$ [yr^{-1}]	η (calculated)	Transition time: $\tau = 2\pi/(\Phi\nu_b)$ [yr]	τ (calculated)
E. acoroides	0.261	0.118 (0.004)	0.67	0.49	−0.104	−0.054 (0.005)	24.6	50 (20)
P. oceanica	0.06	0.09 (0.01)	0.63	0.49	−0.024	−0.06 (0.01)	122.5	70 (20)
P. australis	0.524	0.35 (0.04)	0.58	0.48	−0.208	−0.22 (0.02)	32.9	35 (5)
A. antartica	0.168	0.163 (0.005)	0.63	0.46	−0.067	−0.09 (0.01)	44.6	50 (20)
T. ciliatum	0.422	0.35 (0.03)	0.58	0.48	−0.169	−0.18 (0.01)	28.4	30 (10)
H. uninervis	0.452	0.39 (0.04)	0.68	0.48	−0.180	−0.19 (0.01)	14.5	15 (5)
Z. marina	1.587	1.26 (0.05)	0.57	0.49	−0.635	−0.81 (0.01)	3.4	8 (2)
C. nodosa	2.30	2.31 (0.07)	0.59	0.51	−0.920	−1.33 (0.04)	3.4	4 (1)
H. tasmanica	7.69	3.2 (0.9)	-	0.50	−3.077	−2.2 (0.5)	0.8	2 (1)

able agreement between the predicted and simulated branching frequency (Fig. 7, Table 2). During this growth regime, the observed patches, containing less than 10^3 shoot units, are highly ramified (Fig. 5), with a dendritic morphology that is characteristic of those structures generated by a DLA process (Witten and Sander 1981).

The main feature of a DLA process is that branched or ramified structures are generated. These structures extend in space with a characteristic radius larger than the typical radius of a compact structure composed of the same number of units. In mathematical terms, the characteristic radial size of the aggregates (R) scales with a power law of the number of individuals (N) is $R \sim N^\alpha$, with the exponent α as the inverse of the so-called fractal dimension D_f of the branched structure. For DLA aggregates the fractal dimension has been found to be $D_f = 1.7$ (Witten and Sander 1981), so $\alpha = 1/D_f = 0.59$. This exponent is in agreement with the observed relationship between the radial patch size and the number of living shoots for small clones containing less that 10^3 shoots, which shows a power slope of about 0.6 (Fig. 6, Table 2).

The structure for large clones ($> 10^5$ units) is completely different. The empty areas left during the early stages of clonal extension have been filled to yield compact structures (Fig. 5). At the stage at which the shape of the clones have shifted from complex dendritic structures to more compact geometric structures (circular to oval), the number of units contained in each clone grows with a linear extension given by the characteristic radial patch size, that is, $N \sim R^2$. The fractal dimension is just the Euclidean dimension $D_f = d = 2$ and $\alpha = 0.5$. This result is consistent with the observed relationship between the radial patch size and the number of living shoots for clones containing more than 10^5 units, which shows a 0.5 power scaling (Fig. 6, Table 2). Growth of the clones takes place mainly

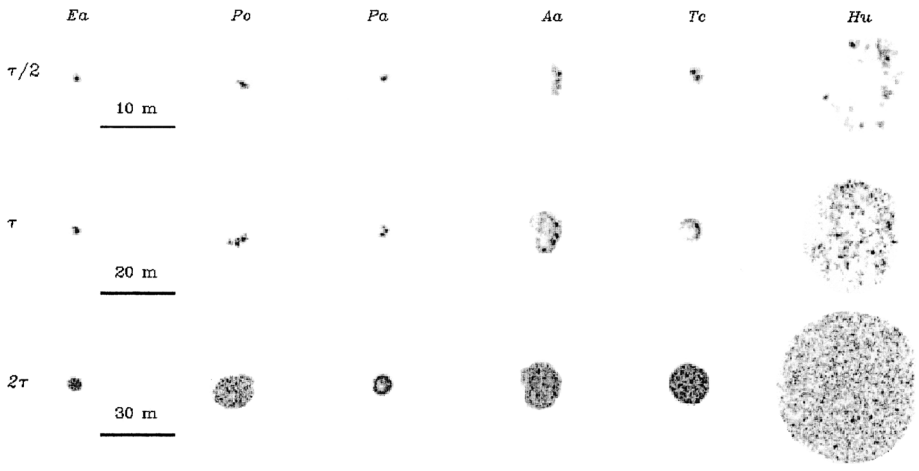

Fig. 5. Snapshots of the shoot density for six selected species at different times. Top row: half of the measured time to the regime shift ($\tau/2$; see Table 2), middle row: at the regime shift (τ), and bottom row: at twice the time to the regime shift (2τ). As indicated in the figure, different length scales apply to each selected time. Labels identify the selected species as in Fig. 1.

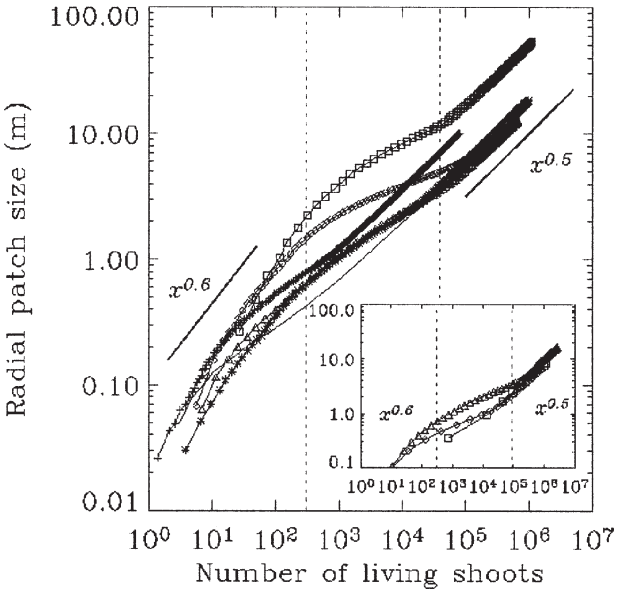

Fig. 6. The increase in the radial patch size with the increasing number of living shoots. Vertical dashed lines separate the two growing regimes: a diffusion limited following a power law with exponent $\alpha = 0.6$, and a compact radial growth with $\alpha = 0.5$. Symbols refer to species: Ea (+), Po (*), Pa (−), Aa (◇), Tc (Δ), and Hu (□). Inset plot includes the behavior of the fastest growing: Zm (◇), Cn (Δ), and Ht (□). Labels are as in Fig. 1.

along the perimeter of the patch, usually referred to as the active zone in the context of pattern formation models. These features conform to the main characteristics of the Eden growth model (Eden 1961) and identify the growth mode of older patches. At the time the clone reaches this compact growth, the growth rate of the clone, which increased continuously during the DLA growth mode, reaches a steady-state value (Fig. 2) close to its rhizome elongation rate, and the shoot and apex density reach a plateau (Fig. 1).

The growth efficiency of the clones, defined as the ratio between the characteristic linear extension of the clones and the total rhizome length produced, during the DLA regime will change in time as:

$$\text{Efficiency} = R_g(t) \Big/ N_s(t) \sim N_s^{(\alpha - 1)} \sim \exp((\alpha - 1)\nu_b t) \quad (4)$$

We define a characteristic efficiency decay rate as $\eta = (\alpha - 1)\nu_b$. We have computed the theoretical expected value of η at the initial stages of the patch growth, where the total rhizome length produced grows exponentially with the branching frequency is found to be valid, and where $\alpha = 0.59$. The predicted value of η derived for the different species modeled can be compared with the value

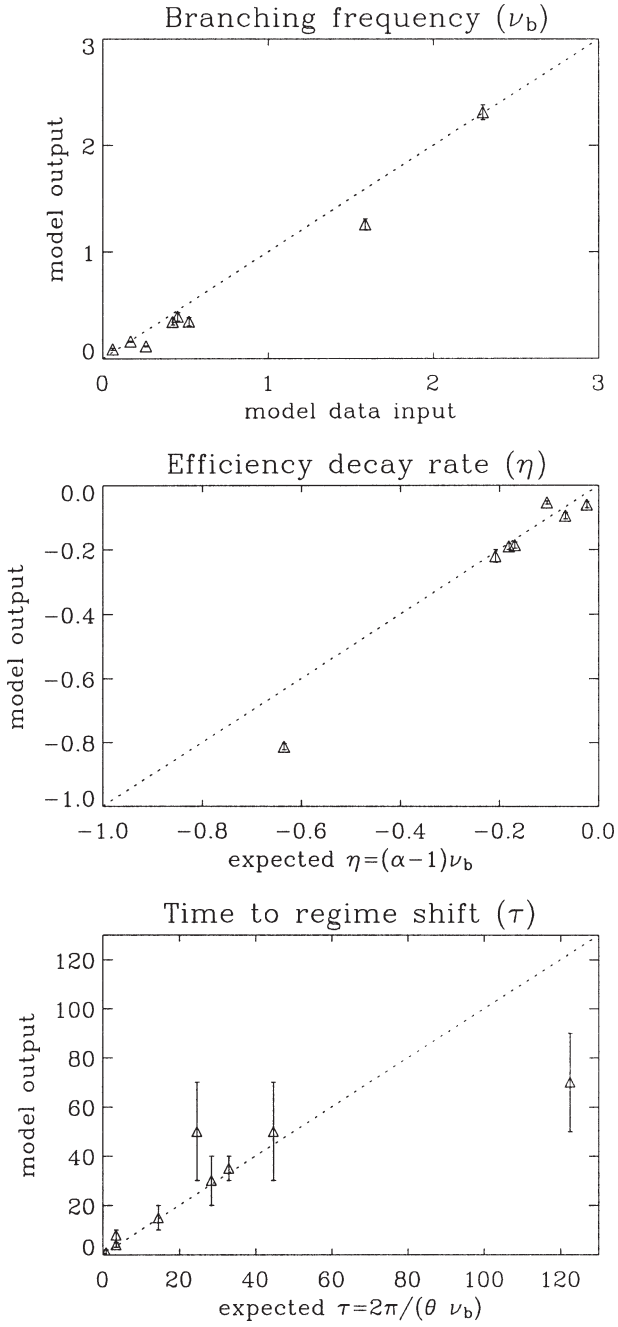

Fig. 7. The relationships between the observed branching frequency (Table 1) and that calculated as the initial slope between the total number of shoots produced by the clone and clonal age (Fig. 3); the rate of decline in growth efficiency (η) predicted from the observed exponent α and the branching frequency ν_b, and the rate of decline derived from the model output (Table 2); the age at which the clones undergo regime shift (τ) predicted from the branching angle (in radians) and frequency and that derived from the model output (Table 2). Data points represent average (± SE) of model output for each species.

derived from the model output by computing the slope in a semi-log plot of the efficiency versus age at the early stages of growth (Table 2). This comparison shows a reasonable agreement between the expected and simulated η values (Fig. 7).

During the early growth period, the patch shape showed an elongated, loosely packed shape, progressing to reach a compact shape as the patch shifted from a diffusion limited to a compact growth mode. The critical event accounting for this change in growth mode is the requirement that patch growth must progress from an initial, random directional growth to a uniform centrifugal growth. This change requires sufficient branching events within the clone as to allow a 180° shift from the initial direction of clone propagation for some of the meristems. With an average branching rate ν_b, the alternate branching mode of the seagrass species modeled (Hemming and Duarte 2000), and branching angle Φ, the time scale required for this 180° shift from the initial direction of the clone propagation can be estimated as:

$$\tau = \frac{2\pi/\Phi}{\nu_b} \quad (5)$$

The predicted theoretical transition time between the diffusion limited to a compact growth mode (Eq. 5) for the set of species modeled is in good agreement with that inferred from the model output (Fig. 7, Table 2), estimated as the average time at which each of the species reaches its steady-state growth rate and shoot and apex density plateau value. Knowledge of the average branching rate ν_b and the branching angle Φ allows for the prediction of the time at which the clones of seagrass species reach their maximum growth rate, characterized by a centrifugal radial patch growth in all directions and the development of compact patch structures. Since these components of seagrass clonal growth are known for most species (Marbà and Duarte 1998), these predictions can be formulated a priori for almost the entire seagrass flora.

In ecological terms, the difference in clonal growth form between the early, dendritic patterns and the compact growth of more developed patches corresponds to the strategies referred to as guerrilla and phalanx (Lovett-Doust 1981). The guerrilla and phalanx strategies are the extremes of a continuum of growth form from production of widely spaced ramets (guerrilla growth form), maximizing interspecific contacts and infiltrating the surrounding vegetation, to the tight-packed advancing front of ramets (phalanx growth form), with high intraclonal contacts that exclude other plants from the clonal territory (Lovett-Doust 1981). Whereas the guerrilla and phalanx strategies have been assumed to be species-specific traits, our model results indicate that these strategies in fact represent chronological stages during clonal development and that, provided sufficient time, all seagrass species transit from clones displaying a guerrilla growth to clones displaying a phalanx growth. The time required for any given species to transit from one mode to another varies across species, with an inverse relationship to their branching rate ν_b and angle Φ (Eq. 3). Species that combine shallow branching angles with low branching rates, such as the slow growing species *P. oceanica* (Table 1), which is the dominant species in developed meadows in the Mediterranean sea (den Hartog 1970), shall maintain a guerrilla growth pattern along considerable (years to decades) time scales. Species that combine wide branching angles with high branching rates shall display a phalanx growth form soon after patch initiation (one to a few years). Variability in the traits that control the duration of the guerrilla phase of clonal growth, i.e., branching rate and angle, can also be considerable within species (Marbà and Duarte 1998). There should also be important variability in the transition from guerrilla to phalanx growth and the perceived ecological strategies within populations of any one species.

The shape and growth of seagrass clones in nature can also be constrained by disturbances affecting plant survival and growth. The growth of *C. nodosa* patches colonizing submerged dunes has been shown to be stimulated towards the direction of dune migration (Marbà et al. 1994). Sand deposition also constrains the progression of the front of *Halodule wrightii* meadows (Bell et al. 1999).

The modeling exercise presented here confirms the complex, nonlinear dynamics of clonal growth for seagrass species that can be derive from internal dynamics of space occupation by the clones, imposing a transition from a DLA, dendritic patch growth to a compact patch growth once internal recolonization of gaps within the clone begins. The time for this transition to occur can be predicted from simple traits, the branching angle, and frequency of the species, and it varies from 1 yr to several decades among species. As a consequence the growth behavior and the apparent growth strategy of the species changes along the development of the clones. The recognition of internally-imposed, nonlinear growth dynamics within seagrass clones may help understand the complex behavior observed during seagrass colonization (Vidondo et al. 1997; Kendrick et al. 1999) and help forecast seagrass colonization.

Acknowledgments

This research is supported by the projects EVK3-CT-2000-00044 and LIFE 2000/NAT/E/7303 funded by the European Commission, and the projects REN2000–2123-E and BFM2001-034-C02-01 funded by the Spanish Ministry of Science and Technology.

Literature Cited

Bell, A. D. 1979. The hexagonal branching pattern of rhizomes of *Alpinia speciosa* L. (Zingiberaceae). *Annals of Botany* 43:209–223.

Bell, A. D. and P. B. Tomlinson. 1980. Adaptive architecture in rhizomatous plants. *Biological Journal of Linean Society* 80:125–160.

Bell, S. S., B. D. Robbins, and S. L. Jensen. 1999. Gap dynamics in a seagrass landscape. *Ecosystems* 2:493–504.

Brouns, J. J. W. M. 1986. Growth patterns in some Indo-West-Pacific seagrasses. *Aquatic Botany* 28:39–61.

Bunde, A. and S. Havlin. 1996. Fractals and Disordered Systems, 1st edition. Springer-Verlag, New York.

Callaghan, T. V., B. M. Svensson, H. Bowman, D. K. Lindley, and B. Å. Carlsson. 1990. Models of clonal plant growth based on population dynamics and architecture. *Oikos* 57:257–269.

den Hartog, C. 1970. The seagrasses of the world. North Holland publishing company, Amsterdam, The Netherlands.

Duarte, C. M. 1995. Submerged aquatic vegetation in relation to different nutrient regimes. *Ophelia* 41:87–112.

Duarte, C. M., M. A. Hemminga, and N. Marbà. 1996. Growth and population dynamics of *Thalassodendron ciliatum*. *Aquatic Botany* 55:1–11.

Duarte, C. M. and K. Sand-Jensen. 1990. Seagrass colonization: Patch formation and patch growth in *Cymodocea nodosa*. *Marine Ecology Progress Series* 65:193–200.

Eden, M. 1961. A two dimensional growth process, p. 223–239. *In* J. Neyman (ed.), 4th Berkeley Symposium on Mathematics, Statistics and Probability, Volume IV: Biology and the Problems of Health. University of California Press, Berkeley, California.

Fonseca, M. S., P. E. Withfield, W. J. Kenworthy, D. R. Colby, and B. E. Julius. 2004. Use of two spatially explicit models to determine the effect of injury geometry on natural resource recovery. *Aquatic Conservation: Marine and Freshwater Ecosystems* 14:1–18.

Hemminga, M. A. and C. M. Duarte. 2000. Seagrass Ecology, 1st edition. Cambridge University Press, Cambridge, Massachusetts.

Jullien, R. and R. Botet. 1985. Scaling properties of the surface of the Eden model in d = 2,3,4. *Journal of Physics A* 18: 2279–2287.

Kendrick, G., J. Eckersley, and D. I. Walker. 1999. Landscape-scale changes in seagrass distribution over time: A case study from Success Bank, Western Australia. *Aquatic Botany* 65:293–309.

Lovett-Doust, L. 1981. Population dynamics and local specialization in a clonal perennial (*Rannunculus repens*). I. The dynamics of ramets in contrasting habitats. *Journal of Ecology* 69:743–755.

Marbà, N. and C. M. Duarte. 1998. Rhizome elongation and seagrass clonal growth. *Marine Ecology Progress Series* 174:269–280.

Marbà, N., J. Cebrián, S. Enrquez, and C. M. Duarte. 1994. Migration of large-scale subaqueous bedforms measured using seagrasses (Cymodocea nodosa) as a tracers. *Limnology and Oceanography* 39:126–133.

Marbà, N., C. M. Duarte, J. Cebrián, S. Enríquez, M. E. Gallegos, B. Olesen, and K. Sand-Jensen. 1996. Growth and population dynamics of *Posidonia oceanica* in the Spanish Mediterranean coast: Elucidating seagrass decline. *Marine Ecology Progress Series* 137:203–213.

Marbà, N. and D. I. Walker. 1999. Population dynamics of temperate Western Australian seagrasses: Importance of growth and flowering for meadow maintenance. *Marine Ecology Progress Series* 184:105–118.

Molenaar, H., D. Barthélémy, P. de Reffye, A. Meinesz, and I. Mialet. 2000. Modelling architecture and growth patterns of *Posidonia oceanica*. *Aquatic Botany* 66:85–99.

Olesen, B. and K. Sand-Jensen. 1994. Demography of shallow eelgrass (*Zostera marina*) populations: Shoot dynamics and biomass development. *Journal of Ecology* 82:379–390.

Sintes, T., N. Marbà, C. M. Duarte, and G. Kendrick. 2005. Non-linear processes in seagrass colonisation explained by simple clonal growth rules. *Oikos* 108:165–175.

Stanley, H. E. and N. Ostrowsky. 1986. On Growth and Form, 1st edition. Martinus Nijhoff, Dodrecht, The Netherlands.

Tomlinson, P. B. 1974. Vegetative morphology and meristem dependence. The foundation of productivity in seagrasses. *Aquaculture* 4:107–130.

Vermaat, J., N. Agawin, C. M. Duarte, M. D. Fortes, N. Marbà, and J. Uri. 1995. Meadow maintenance, growth and productivity of a mixed Philippine bed. *Marine Ecology Progress Series* 124:215–225.

Vidondo, B., A. L. Middleboe, K. Stefansen, T. Lützen, S. L. Nielsen, and C. M. Duarte. 1997. Dynamics of a patchy seagrass (*Cymodocea nodosa*) landscape. Size and age distributions, growth and demography of seagrass patches. *Marine Ecology Progress Series* 158:131–138.

Witten, T. A. and L. M. Sander. 1981. Diffusion-limited aggregation, a kinetic critical phenomenon. *Physical Review Letters* 47:1400–1403.

Received, September 7, 2004
Revised, August 12, 2005
Accepted, September 30, 2005